Photophysiology of the haploid form of the cryptophyte Teleaulax amphioxeia

Sarah Garric, Morgane Ratin, Benoit Gallet, Johan Decelle, Ian Probert, Francisco Rodriguez, Christophe Six

▶ **To cite this version:**

Sarah Garric, Morgane Ratin, Benoit Gallet, Johan Decelle, Ian Probert, et al.. Photophysiology of the haploid form of the cryptophyte Teleaulax amphioxeia. Journal of Phycology, 2024, 60 (5), pp.1220-1236. ⟨10.1111/jpy.13495⟩. ⟨hal-04781170⟩

HAL Id: hal-04781170

https://hal.science/hal-04781170v1

Submitted on 13 Nov 2024

HAL is a multi-disciplinary open access archive for the deposit and dissemination of scientific research documents, whether they are published or not. The documents may come from teaching and research institutions in France or abroad, or from public or private research centers.

L'archive ouverte pluridisciplinaire **HAL**, est destinée au dépôt et à la diffusion de documents scientifiques de niveau recherche, publiés ou non, émanant des établissements d'enseignement et de recherche français ou étrangers, des laboratoires publics ou privés.

Distributed under a Creative Commons CC BY-NC-ND 4.0 - Attribution - Non-commercial use - No Derivative Works - International License

Photophysiology of the haploid form of the cryptophyte *Teleaulax amphioxeia* strain Cr10EHU

Sarah Garric[1], Morgane Ratin[1], Benoit Gallet[2], Johan Decelle[3], Ian Probert[4], Francisco Rodriguez[5] & Christophe Six[1*].

[1] Sorbonne Université, Centre National de la Recherche Scientifique, UMR 7144 « Adaptation et Diversité en Milieu Marin », group « Ecology of Marine Plankton », Station Biologique de Roscoff, 29680 Roscoff, France.

[2] Commissariat à l'Énergie Atomique et aux Énergies Alternatives, UMS3518, Integrated Structural Biology, 71 avenue des Martyrs, 38042 Grenoble Cedex 9, France.

[3] Centre National de la Recherche Scientifique, Laboratoire de Physiologie Cellulaire & Végétale, Commissariat à l'Energie Atomique, 17, avenue des Martyrs, 38 054 Grenoble cedex 9, France.

[4] Centre National de la Recherche Scientifique, Fédération de Recherche 2424, Station Biologique de Roscoff, 29680 Roscoff, France.

[5] Instituto español de oceanografia, subida a radio faro, 50., Vigo 36390, Spain.

Running title: Photophysiology of *Teleaulax amphioxeia*

* **To whom correspondence should be addressed**: Christophe Six, six@sb-roscoff.fr

Key words: Cryptophyte, *Teleaulax*, *Plagioselmis*, light, photosynthesis, photoacclimation

We certify that there is no conflict of interest associated with this manuscript.

Abstract (200 words)

Cryptophytes are abundant and ubiquitous microalgae that constitute a major plastid source for ciliates and dinoflagellates. Despite their ecological significance, the understanding of their light preferences and photophysiology remains limited. We provide a comprehensive study of the response of the haploid strain *Teleaulax amphioxeia* Cr10EHU to varying light irradiance. This strain is capable of growing under a wide range of irradiance levels, notably by finely tuning the different pigments bound to the membrane light-harvesting proteins. The cell content in the luminal phycoerythrin, identified as the major photosynthetic antenna, revealed to be highly flexible. Microscopy analyses unveiled that under low growth light, phycoerythrin accumulated in large thylakoidal vesicles likely allowing efficient green photon capture. *Teleaulax amphioxeia* Cr10EHU effectively regulated light utilization by using a mechanism akin to the state transition process, with a larger amplitude observed under high growth irradiance. Furthermore, our results revealed the establishment of permanent, irradiance-dependent non-photochemical quenching of fluorescence, facilitating the dissipation of excess light. This study underscores the particularities and the significant photoadaptability of the plastid of the haploid form of *Teleaulax amphioxeia*. It constitutes a comprehensive photophysiological characterization of the Cr10EHU strain that paves the way for future laboratory studies of the kleptoplastidy process.

Introduction

Cryptophytes are unicellular biflagellate protists (~5-50 µm) that are widely distributed in all illuminated aquatic environments. They are notably abundant and ubiquitous in the World Ocean, as revealed by a number of metabarcoding studies (see e.g. Caracciolo et al., 2022; Hamilton et al., 2021; Pierella Karlusich et al., 2020; Xin et al., 2023). With the exception of the heterotrophic genus *Goniomonas*, cryptophytes are obligatory phototrophs that have acquired their plastids through secondary endosymbiosis from an ancient group of red algae. This endosymbiotic process has notably resulted in the plastids being enclosed by four membranes, and the presence of a vestigial red algal genome called nucleomorph (Archibald, 2015; Baurain et al., 2010; Keeling, 2013).

Cryptophytes form a monophyletic group of about 20 genera and 200 described species (Cerino and Zingone, 2007; Clay et al., 1999). Among the species of the so-called *Plagioselmis*/*Teleaulax*/*Geminigera* (PTG) clade, *Plagioselmis prolonga* and *Teleaulax amphioxeia* show some distinctive phenotypic and ecological traits but have been identified as the haploid and diploid forms of the same organism, respectively (Altenburger et al., 2020). This organism, referred hereafter to as *Teleaulax amphioxeia*, is a widely distributed cryptophyte recognized as an important donor of plastids to ciliates of the genus *Mesodinium* (Hansen et al., 2012), which are in turn preys for *Amylax* and *Dinophysis* dinoflagellates (Hansen et al., 2013; Koike and Takishita, 2008; Park et al., 2013). Several studies conducted on natural populations have highlighted the crucial role of *Teleaulax amphioxeia* as a food source, as plastids found in *Mesodinium rubrum* and *Dinophysis acuminata* are most predominantly derived from this cryptophyte species (Peltomaa and Johnson, 2017; Rial et al., 2015). Additionally, observations have revealed that the widely distributed *Mesodinium rubrum* can utilize plastids from various *Teleaulax* species but cannot utilize plastids from other genera of cryptophytes (Hansen et al., 2012; Peltomaa and Johnson, 2017).

Light utilization by plastids relies primarily on the light absorption process and cryptophytes utilize two types of photosynthetic antennae that funnel light energy towards the photosystem reaction centers. The 'Light Harvesting Complex' (LHC) proteins are intrinsic to the plastidial thylakoid membranes and are directly associated with the reaction centers of both photosystems (PS; Büchel, 2020). These proteins bind chl *a* and chl c_2, as well as an original composition of carotenoids devoid of epoxydic compounds (Pennington et al., 1985), whose functions are still poorly understood (Greenwold et al., 2019; Kereïche et al., 2008; Šebelík et al., 2020; Zhao et al., 2023). However, the major antenna protein in cryptophytes is extrinsic to the thylakoids and consists of a phycobiliprotein that is partially inherited from the red algal plastid ancestor (Rathbone et al., 2021). While cyanobacteria and red algae link phycobiliproteins together to form a large antenna complex known as the phycobilisome, cryptophyte species possess only one phycobiliprotein, which is freely present

in the thylakoid lumen (Ludwig and Gibbs, 1989). Noteworthy, the distinct cryptophyte lineages have evolved a variety of these phycobiliproteins, which may bind different combinations of phycobilin pigments (Greenwold et al., 2019; Richardson, 2022). About eight types of cryptophyte phycobiliproteins have been so far described, named according to their absorption maximum (Cunningham et al., 2019; Hoef-Emden and Archibald, 2017). In marine cryptophytes such as *Teleaulax amphioxeia*, the most common phycobiliprotein is phycoerythrin (PE) 545.

Compared to other phytoplankton groups, the ecological niches of cryptophytes have been poorly studied. Regarding their light niches, several authors have acknowledged that cryptophytes are adapted to low-light environments, as evidenced by their efficient use of green light through phycobiliproteins, because green light is often abundant at deeper depths where irradiance is low (Hoef-Emden and Archibald, 2017). However, it is important to note that coastal and offshore waters exhibit distinct wavelength differences that are not solely dependent on depth. Coastal waters provide a greater abundance of green wavelengths to phytoplankton compared to offshore waters. Consequently, it is often challenging to disentangle the effects of light irradiance from those of light spectral quality in marine environments. Moreover, the mechanisms that underly the regulation of light utilization in cryptophyte microalgae, such as light harvesting and photoprotection, have been significantly underexplored and there is an urgent need for comprehensive laboratory studies to investigate the photophysiological capacities of these ecologically significant organisms. The case of *Teleaulax amphioxeia* is particularly interesting because the ciliates and dinoflagellates that host their plastids undergo significant diel vertical migration of tens of meters in the water column (Moeller and Johnson, 2023). This suggests that *Teleaulax amphioxeia* plastids may possess highly adaptable photoacclimation capacities, enabling them to thrive in very different light irradiance niches.

To gain a deeper understanding of the possible light irradiance niches inhabited by cryptophytes and the organisms that harbor their plastids, we here present a comprehensive study of the photophysiological response to light irradiance levels of the haploid, '*Plagioselmis* stage' of the strain *Teleaulax amphioxeia* Cr10EHU. This strain is frequently used in laboratory studies involving the ciliate *Mesodinium* and the toxic dinoflagellate *Dinophysis*, whose culture methods and health rely on the physiological status of the cryptophyte. Our study unveils the remarkable photophysiological adaptability of *Teleaulax amphioxeia* Cr10EHU and sheds light on distinct photoacclimation characteristics of its plastid.

Material & methods

Biological material and culture conditions

The haploid strain *Teleaulax amphioxeia* Cr10EHU, initially called *Plagioselmis prolonga* Cr10EHU, was isolated in 2003 in the estuary of the Nervión River of Bilbao, in Spain (GPS Coordinates: 43.295699, -2.974471) the 2003/09/03. The environmental conditions at the isolation site were: temperature: 21°C; salinity: 19.8 psu; pH: 7.6; oxygen concentration: 4.1 mg L^{-1}. *Teleaulax amphioxeia* Cr10EHU was grown in vented polycarbonate flasks filled with L1 medium (Guillard and Hargraves, 1993). The cultures were maintained in exponential growth phase in temperature-controlled chambers (Lovibond) at 19°C, under different irradiances of continuous white light provided by multicolor LED systems (EasyLED).

Sequencing and Phylogenetic analyses

An exponentially growing culture of the Cr10EHU strain (10 mL) was harvested by centrifugation and DNA extraction was immediately carried out using E.Z.N.A.® Soil DNA Kit (Omega Bio-tek Inc., USA) following manufacturer's instructions. The whole 18S SSU rRNA gene was amplified using the pair of primers EUKA/EUKB (Medlin et al., 1988) following previously described procedure (Sunesen et al., 2020). The amplicons were purified with ExoSAP-IT (USB Corporation, Cleveland, Ohio, USA) and sequenced using Macrogen sequencing service (Seoul, Korea). The SSU rDNA sequences were aligned using CLUSTALW multiple alignment in MEGA X (Kumar et al., 2018), and both amplicons manually curated to yield the final sequence (1607 bp ; Accession # OR782920).

The phylogenetic tree was built using the Cr10EHU strain sequence and SSU rRNA sequences downloaded from GenBank, selected to show the different Cryptophyte lineages with a focus on the PTG group, and with the Katablepharids as outgroup (Table S1). After ClustalW alignment in Bioedit 7.2.5 (Hall, 2007), the matrix data consisted in 58 sequences of 1663 base pairs including gaps. Bayesian and maximum likelihood analyses were carried out using a GTR family model with gamma distribution and invariant sites (+G+I). Maximum likelihood analysis was performed using MEGA 10.2.6 (Kumar et al., 2018) and bootstrap values were calculated from 1000 replicates. Bayesian inference were performed using MrBayes 3.2.6 (Ronquist and Huelsenbeck, 2003) as implemented in the software Geneious Prime 2022.2.1, with four Markov Chain Monte Carlo runs for one million generations. A tree was sampled every 1000 generations and 25 % of trees were discarded as burn-in. The presented tree topology is based on the Bayesian analysis. The node supports are indicated with posterior probabilities of Bayesian analysis alongside with the bootstrap values of the maximum likelihood analysis.

Flow cytometry

The cell density was measured using a high-sensitivity cytometer (Novocyte Advanteon, Agilent). Growth rates were computed as the slope of a ln(Nt) versus time plot, where Nt is the cell density at time t. Forward and side scatters as well as red (695/40 nm) and orange (572/28 nm) cell fluorescences were measured upon laser excitation at 488 nm and the values were normalized to the signal emitted by standard 3 µm fluorescent beads.

Pulse Amplitude Modulated fluorimetry

PAM measurements were carried out with a multi-wavelength fluorimeter PHYTO-PAM II (Walz), whose cuvette holder was maintained at 19°C.

PSII maximal quantum yield and state transition like mechanisms - After 5 min incubation in the dark, the modulated light (2 Hz) was switched on and the basal fluorescence level F_0 was recorded. After triggering a saturating multiple light pulse (400 ms, 2000 µmol photons m^{-2} s^{-1}) yielding the F_{Mdark} fluorescence level, actinic light was turned on in the presence of 100 µM 3-(3,4-dichlorophényl)-1,1-diméthylurée (DCMU). After signal stabilization, the maximal fluorescence level F_M was recorded and the PSII maximal quantum yield was calculated as:

$$(F_V/F_M) = (F_M - F_0)/F_M$$

The state transition-like mechanism (Cheregi et al., 2015) was conceptualized as a non-photochemical quenching of fluorescence parameter, NPQ_{ST}, calculated between the dark-acclimated and the light/DCMU states as:

$$NPQ_{ST} = (F_M - F_{Mdark})/F_{Mdark}$$

PSII effective absorption cross-section for green light - Dilute culture aliquots were incubated 2 min under weak far-red light inducing no significant PSII excitation and oxidizing the plastoquinone pool through PSI excitation. Single turnover pulses of green light (80 µs; 2400 µmol photons m^{-2} s^{-1}, 540 nm) were triggered to record O-I_1 fluorescence fast kinetics. The induction curves were modelled and the PSII cross-section $\sigma(II)_{540nm}$ was calculated using the Phytowin 3 software (Schreiber et al., 2012).

PSII electron transport curves and non-photochemical quenching of fluorescence - After the measurement of the F_0 fluorescence level, 14 steps of 60 s increasing light irradiance were applied to the sample. The instantaneous F_t and maximal F_M' fluorescence levels were measured at the end of each step by triggering a multiple turnover saturating pulse. The PSII electron transport rate, ETRII (e^- $PSII^{-1}$ s^{-1}), was calculated for each step as follows (Schreiber et al., 2012):

$$ETRII = (((F_M'-F_t)/F_M') \times \sigma(II)_{540nm} \times I \times 0.6022)/(F_V/F_M)$$

where I is the instantaneous irradiance at the considered step. ETRII values were plotted against instantaneous irradiance. The initial slope α, reflecting PSII efficiency under non-saturating light, and the optimal irradiance E_{opt} were derived by fitting the photosynthesis Eilers and Peeters (1988) model, using the R package Phytotools 1.0.

Non-Photochemical Quenching of PSII fluorescence (NPQ) was calculated for each irradiance step according to the Stern-Volmer formula:

$$NPQ = (F_M - F_M')/ F_M'$$

The maximal NPQ values reached for each curve, NPQ_{MAX}, were then plotted against growth irradiance.

High-Performance Liquid Chromatography - Volumes of 75 mL culture were harvested by centrifugation at 19°C (8 000 × *g*, 7 min) and stored at −80 °C until analysis. After extraction in cold 90% methanol, the extracts were injected in an HPLC 1100 Series System (Hewlett-Packard) equipped with a C_8 column (Waters). The different pigments were separated according to an adapted procedure of Zapata et al. (2000) and quantified using homemade purified standards. The pigment cell contents were calculated using the flow cytometry cell counts.

Phycoerythrin quantification by in gel-fluorescence - Volumes of 75 mL culture were extracted according to a previously described procedure (Six et al., 2021). Total protein concentration was determined by measuring absorbance at 280 nm and 0.7 µg of total protein per well was loaded on 4-12% acrylamide gradient gels (Invitrogen), along with known quantities of PE standard proteins. The β-PE subunit was quantified by fluorescence within the electrophoresed gels under blue light excitation, using a LAS-4000 imager (GE Healthcare). PE standard proteins were purified by exclusive ion exchange chromatography (AKTA-Start, GE Healthcare) followed by several steps of molecular ultrafiltration (Vivaspin).

Transmission electron microscopy - Mat & Meth Benoit-Johan.

Results

Phylogenetic analysis

Figure 1 shows the 18S rRNA gene phylogeny of 58 cryptophytes sequences, with a particular focus on the genetic diversity of the PTG clade. The overall tree topology is similar to previously published phylogenies (Altenburger et al., 2020; Deane et al., 2002; Hamilton et al., 2021; Laza-Martínez et al., 2012). As expected, the strain Cr10EHU sequence (Accession # OR782920) falls within

the group gathering sequences of both the diploid and haploid forms of *Teleaulax amphioxeia* (clades II and III *sensu* Hamilton et al., 2021).

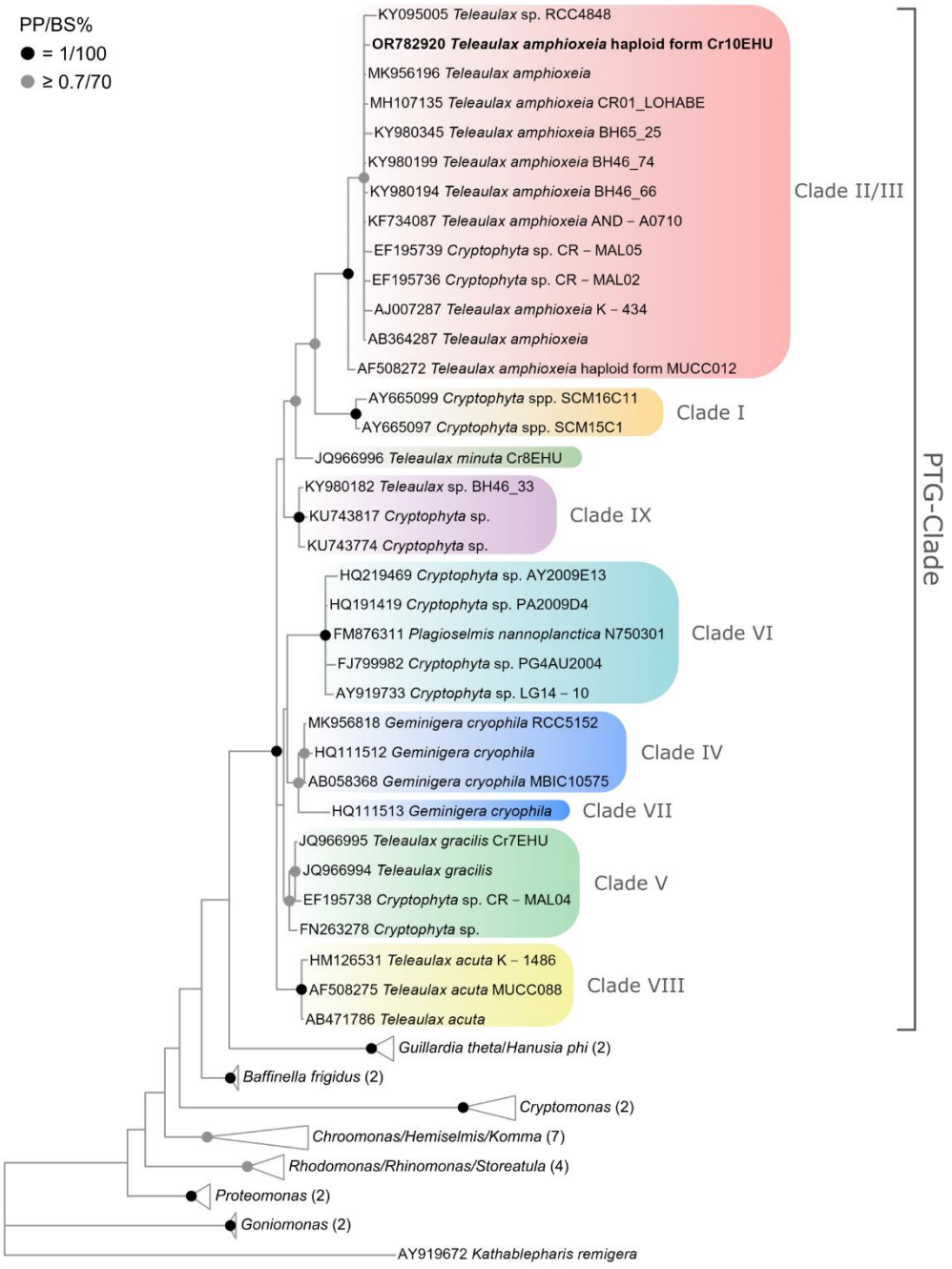

Figure 1: Phylogenetic position of the haploid *Teleaulax amphioxeia* strain Cr10EHU. The 18S rRNA tree topology is based on a Bayesian analysis and the robustness of clades are indicated as posterior probabilities (PP; Bayesian) and bootstrap values (BS; maximum likelihood, 1000 replicates), represented by dark (PP = 1 and BS = 100) or grey circles (PP ≥ 0.7 and BS ≥ 70). The indicated clades of the PTG lineage are *sensu* Hamilton et al. (2021).

Growth and cell features

Teleaulax amphioxeia Cr10EHU was successfully cultivated across a range of light irradiances spanning from 20 to 200 µmol m^{-2} s^{-1}, following gradual acclimation to higher light levels. Notable changes in the color of the culture indicated the induction of active photoacclimation processes (Fig. 2A). The maximum growth rate observed was 1.08 day^{-1}, with growth saturation occurring at 150 µmol m^{-2} s^{-1} (Fig. 2B). Under our culture conditions, the strain exhibited a four-fold increase in growth rate when transitioning from 20 µmol m^{-2} s^{-1} to the highest recorded value.

The light Forward Scatter parameter is commonly used as an indicator of cell biovolume (Marie et al., 2005). In response to increasing light irradiance, the haploid *Teleaulax amphioxeia* Cr10EHU demonstrated a slight 20% increase in this parameter from low to high growth irradiance (Fig. 2C). Similar variations were observed for the Side Scatter parameter, which exhibited an approximate 40% increase across the range of growth irradiances (Fig. 2D).

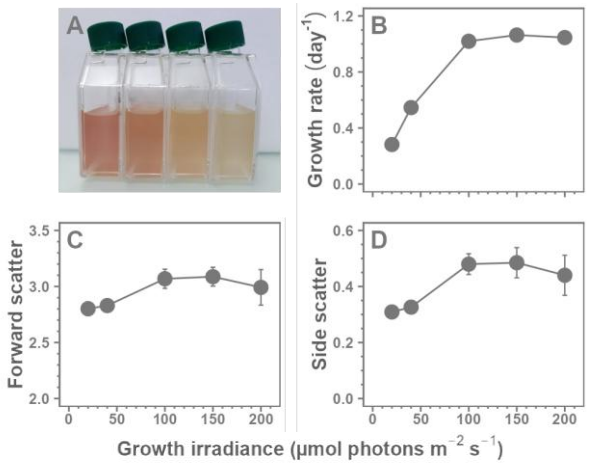

Figure 2: Photos of cultures of the haploid *Teleaulax amphioxeia* Cr10EHU in stationary growth phase, grown at 20, 40, 100 and 200 µmol photons m^{-2} s^{-1} from left to right (**A**). Growth rates (**B**), forward scatter (**C**) and side scatter (**D**) of the haploid *Teleaulax amphioxeia* Cr10EHU grown at different light irradiances (n ≥ 3).

Variations in pigmentation

We studied the changes in pigmentation of the haploid *Teleaulax amphioxeia* Cr10EHU in response to growth light irradiance. HPLC analyses enabled the detection of 8 major membrane pigments, including chl *a*, chl c_2, phaeophytin *a*, alloxanthin, crocoxanthin, α-carotene and two unknown *cis*-xanthophylls (Fig. 3AB, S1). Traces of other unknown xanthophylls were also detected but could not be quantified.

Chl *a* cell content remained stable at 0.40 pg $cell^{-1}$ within the light irradiance range of 20 to 40 µmol m^{-2} s^{-1} and decreased to a plateau at 0.26 pg $cell^{-1}$ starting from 150 µmol m^{-2} s^{-1}, representing a reduction of 35% (Fig. 3C). These findings were corroborated by the *in vivo* red

fluorescence of the cells, as measured by flow cytometry, which exhibited the same variations. With our HPLC system, the chl c_2 appeared as a double peak displaying the exact same absorption properties. We therefore integrated the whole area to determine chl c_2 quantities. The cell content of chl c_2 and crocoxanthin in the cells followed an identical pattern, with a substantial decrease of 65% from low to high growth irradiance (Fig. 3D). Alloxanthin and α-carotene exhibited smaller reductions, of 24% and 28%, respectively, from low to high growth light (Fig. 3E). The ratios of these two carotenoids to chl *a* were nearly constant (Fig. S2). The cell content variations in the two *cis*-xanthophylls displayed distinct patterns. While there was some variability in the results due to the low abundance of these compounds, it appeared that unk1 remained stable, whereas unk2 increased in response to increasing growth light irradiance.

We also measured the PE-545 cell content using a quantitative in-gel fluorescence method (Fig. 3GH). The PE cell content showed a large and continuous 75% decrease with increasing growth light; with no plateau at the lowest nor highest irradiances tested. These results were confirmed by the measurement of the cellular orange fluorescence by flow cytometry, which showed a similar trend.

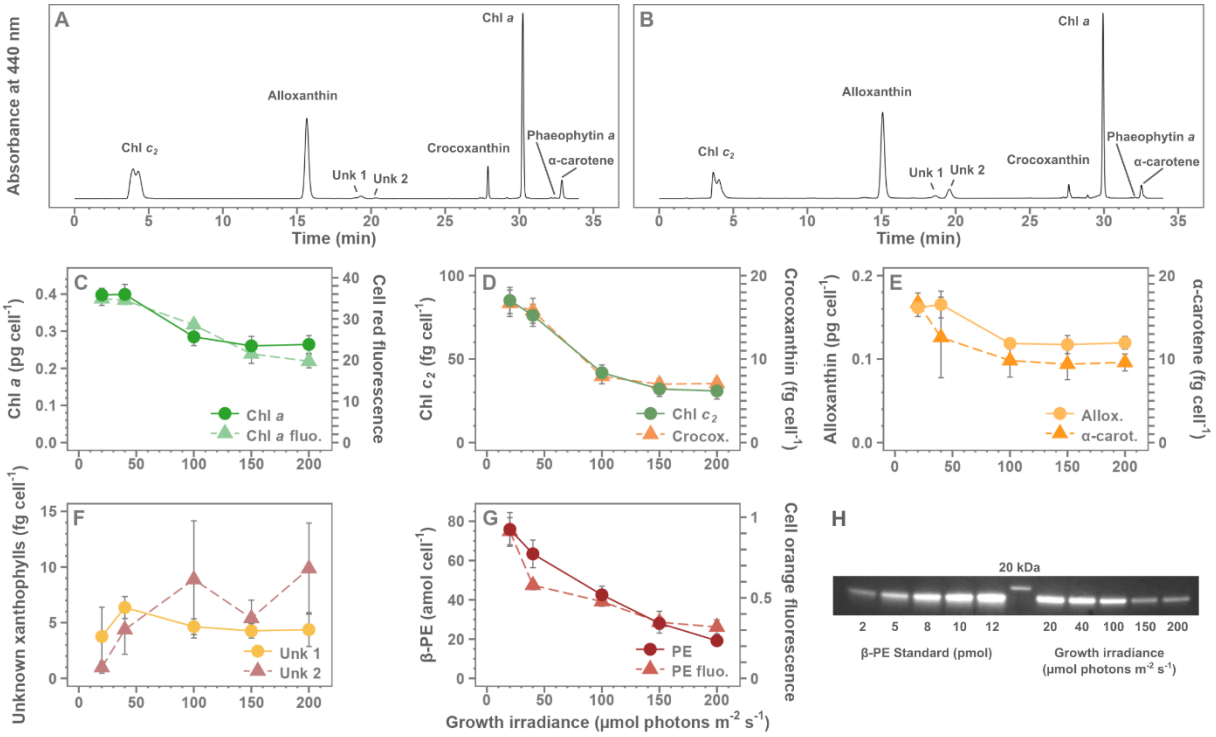

Figure 3: Variations in the pigmentation of the haploid *Teleaulax amphioxeia* Cr10EHU grown under different light irradiances. Representative HPLC chromatograms of cultures grown at 20 (**A**) and 200 (**B**) µmol photons m^{-2} s^{-1}; variations of chl *a* cell content as measured by HPLC (green circles) and cell red fluorescence as measured by flow cytometry (green

triangles; **C**); variations in chl c_2 (green circles) and crocoxanthin (orange triangles; **D**), alloxanthin (orange circles) and α-carotene (orange triangles; **E**) and the two *cis*-xanthophylls (unk1 and unk2; **F**); variations in cell orange fluorescence as measured by flow cytometry and phycoerythrin cell content as measured by in-gel fluorescence (**G**); example of photo of gel used for phycoerythrin fluorescence quantification under blue light excitation (0.7 µg total protein per well), using a purified phycoerythrin-545 standard (**H**; n ≥ 3).

Regulation of photosystem II activity

We measured the maximal PSII quantum yield, F_V/F_M, using a method adapted to organisms that exhibit a state transition mechanism (Fig. 4A), *i.e.* for which it is not possible to record the maximal fluorescence level in a dark-acclimated sample. This method also enabled quantifying of the state transition amplitude in the form of non-photochemical quenching. The F_V/F_M parameter, which represents the maximal proportion of open PSII, showed high values across all tested growth irradiances, with a slight increase from 20 to 100 µmol photons m^{-2} s^{-1} (Fig. 4B). The NPQ_{ST} parameter, a measure of the amplitude of the state transition mechanism, showed a 4-fold increase in response to increasing growth irradiances (Fig. 4C).

Using a single turnover flash method, we measured the variations in the PSII absorption cross-section for green light, $\sigma(II)_{540nm}$, in response to growth light irradiance. In many cryptophytes and other phycoerythrobilin-rich organisms, this parameter indicates the size of the effective phycobiliprotein antenna. In *Teleaulax amphioxeia*, it is mainly influenced by the PE to PSII molar ratio, but also by the efficiency of the excitonic transport among PE proteins and between PE and PSII complexes. The $\sigma(II)_{540nm}$ showed a notable 25% decrease from low to high growth irradiance (Fig. 4D), indicating a downregulation of the effective size of the major PSII antenna in response to increasing growth irradiance.

We generated curves showing the absolute PSII electron transport *versus* instantaneous irradiance for *Teleaulax amphioxeia* Cr10EHU grown under different irradiances (Fig. 4E). Fitting a model to these curves allowed the determination of several classical parameters characterizing PSII functioning. The initial slope of the curves, α, represents the efficiency of the ETRII at instantaneous low irradiances. This parameter was high at 20 and 40 µmol photons m^{-2} s^{-1} but decreased to a 15% lower level at growth lights higher than 100 µmol photons m^{-2} s^{-1} (Fig. 4F). The estimated optimal irradiance E_{OPT}, *i.e.* the instantaneous irradiance at which ETRII is maximal, nearly doubled over the range of growth light irradiances tested (Fig. 4G). These variations of α and E_{OPT} indicate that the curves ETRII/Irradiance saturate at lower irradiance for low light acclimated compared to high light ones. The estimated maximal ETRII, ETR_{MAX}, displayed a 20% increase at higher growth light (Fig. 4H), demonstrating large capacities to optimize ETRII in response to changes in growth irradiance.

Following the ETRII/Irradiance curve protocol, we assessed the variations in global NPQ during the gradual increase of instantaneous irradiance (Fig. S4). At low levels of instantaneous light,

the relaxation of NPQ associated to the state transition mechanism persisted up to 35 µmol photons m^{-2} s^{-1}, irrespective of the growth irradiance. Beyond this point, global NPQ increased until reaching a plateau marking NPQ_{MAX}. This parameter, which can be interpreted as the induction of maximal dissipation of excess light into heat in these conditions, nearly doubled from low growth light to a plateau starting from approximately 100-150 µmol photons m^{-2} s^{-1} (Fig. 4I).

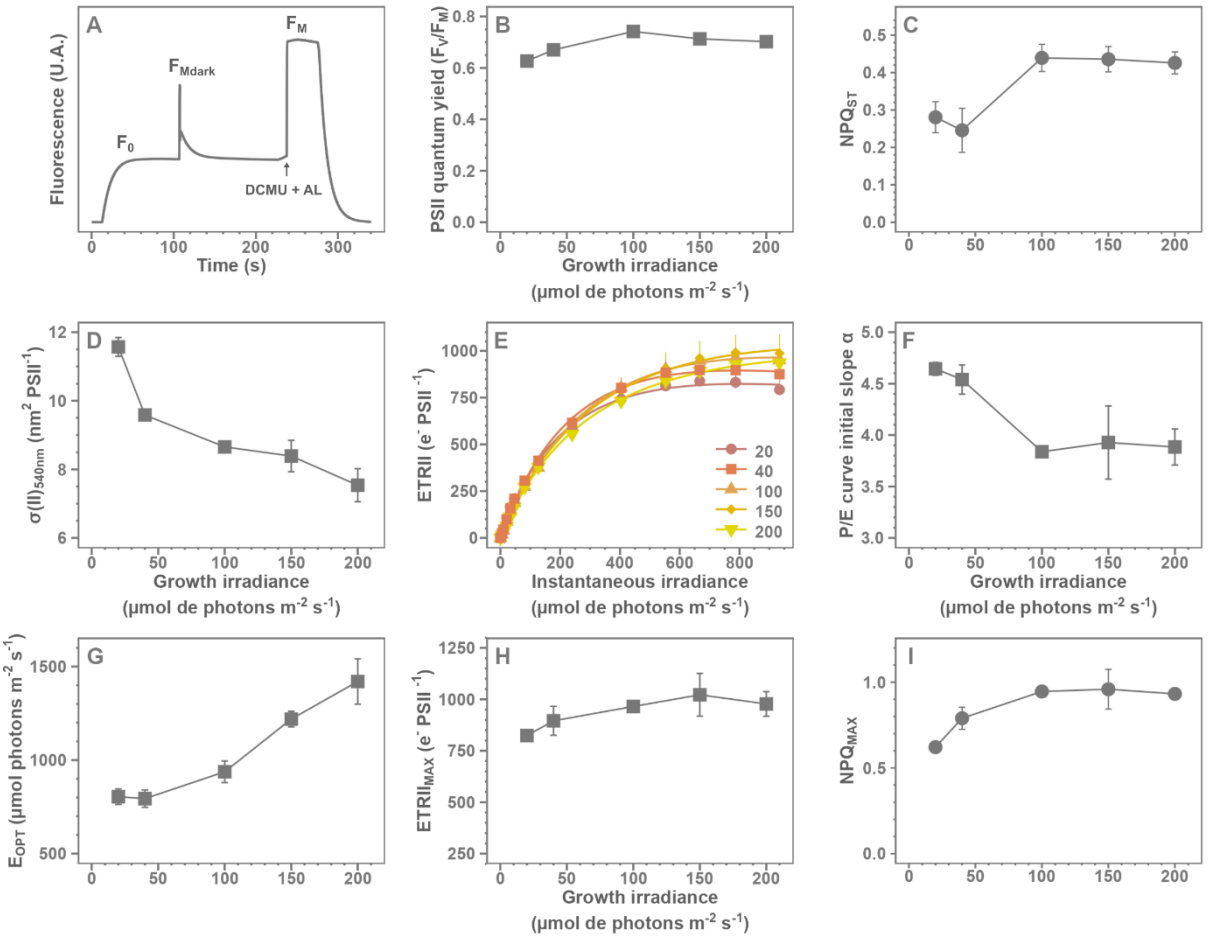

Figure 4: Variations of PAM fluorimetry parameters for the haploid *Teleaulax amphioxeia* Cr10EHU grown at different light irradiances. Representative example of fluorescence trace showing the measurement of the photosystem (PS) II maximal quantum yield, F_V/F_M, and the Non-Photochemical Quenching of fluorescence associated to state transitions, NPQ_{ST}, for a culture acclimated to 100 µmol photons m^{-2} s^{-1} (**A**), maximal PSII quantum yield, F_V/F_M (**B**), state transition amplitude, NPQ_{ST} (**C**), Effective PSII absorption cross-section for green light, $\sigma(II)_{540nm}$ (**D**), PSII absolute Electron Transport Rate *versus* Irradiance curves, with Eilers and Peeters (1988) model fitted (**E**), PSII conversion efficiency at low light irradiance, α (**F**), optimal irradiance for PSII electron transport rate, I_{OPT} (**G**); maximal PSII electron transport rate, $ETRII_{MAX}$ (**H**) and maximal Non Photochemical Quenching of PSII fluorescence, NPQ_{MAX} (**I**; n ≥ 3).

Kinetics of photoacclimation

We investigated the capacities for dynamic photoacclimation of the haploid *Teleaulax amphioxeia* Cr10EHU by shifting cultures acclimated to 150 µmol photons m^{-2} s^{-1} to four lower light irradiances.

Monitoring the $\sigma(II)_{540nm}$ parameters enabled to calculate rates of acclimation of the green light harvesting process. The results showed that *Teleaulax amphioxeia* Cr10EHU efficiently modulated the acclimation rate of $\sigma(II)_{540nm}$ in relation to the extent of the irradiance decrease (Fig. 5). Furthermore, the response was not linear; instead, it exhibited an exponential-like pattern, with much higher rates observed when the cultures were transferred to very low light levels.

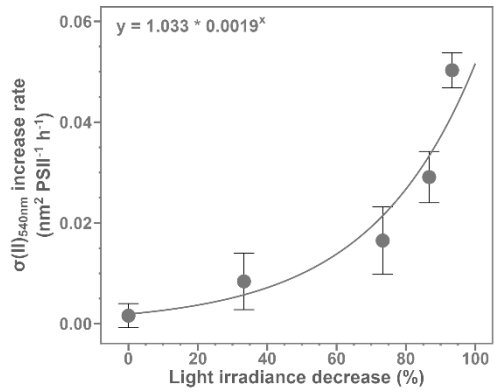

Figure 5: Low light acclimation capacities of *Teleaulax amphioxeia* Cr10EHU grown at 150 µmol photons m^{-2} s^{-1}. The photoacclimation capacities were studied determining the rates of increase in the PSII absorption cross-section for green light in response to different amplitudes of sudden light irradiance decrease (n = 3). Retirer l'équation

Ultrastructural changes in response to growth light irradiance

Cultures of the haploid *Teleaulax amphioxeia* Cr10EHU acclimated to both low and high growth light irradiances were concentrated and used for ultrastructural analyses by transmission electron microscopy. The micrographs showed that the cells of *Teleaulax amphioxeia* Cr10EHU were about 3 x 5 µm and were covered with plates, as expected for the haploid form of this species (Altenburger et al., 2020; Novarino et al., 1994; Fig. 6). Peripheral ejectosome vesicles interrupted the inner periplast component. As previously described for *Teleaulax* species (Deane et al., 2002; Laza-Martínez et al., 2012), the unique plastid was surrounded by four membranes, with the two innermost ones defining the plastid *sensu stricto*. The third membrane delineated a compartment housing the nucleomorph and the starch granules, a positioning consistent with the presence of floridean starch in the cytoplasm of rhodophytes.

When the cells were grown under low light irradiance, the thylakoids never showed any form of clustering and appeared wide, displaying swellings at their extremities (Fig. 6BC). Particularly, the thylakoids situated in the inner region of the plastid, around the pyrenoid region, were noticeably affected by this type of deformation. Swollen thylakoid ends were apparently able to detach from the main thylakoid lamellae to form round-shaped vesicles, containing a substantial amount of material exhibiting high electron density. When grown under high light conditions, the plastids were much thinner than under low light and were localized close to the plasma membrane (Fig. 6D). The

thylakoids were also thinner, formed many less vesicles and were sometimes grouped by three (Fig. 6E).

Low Light

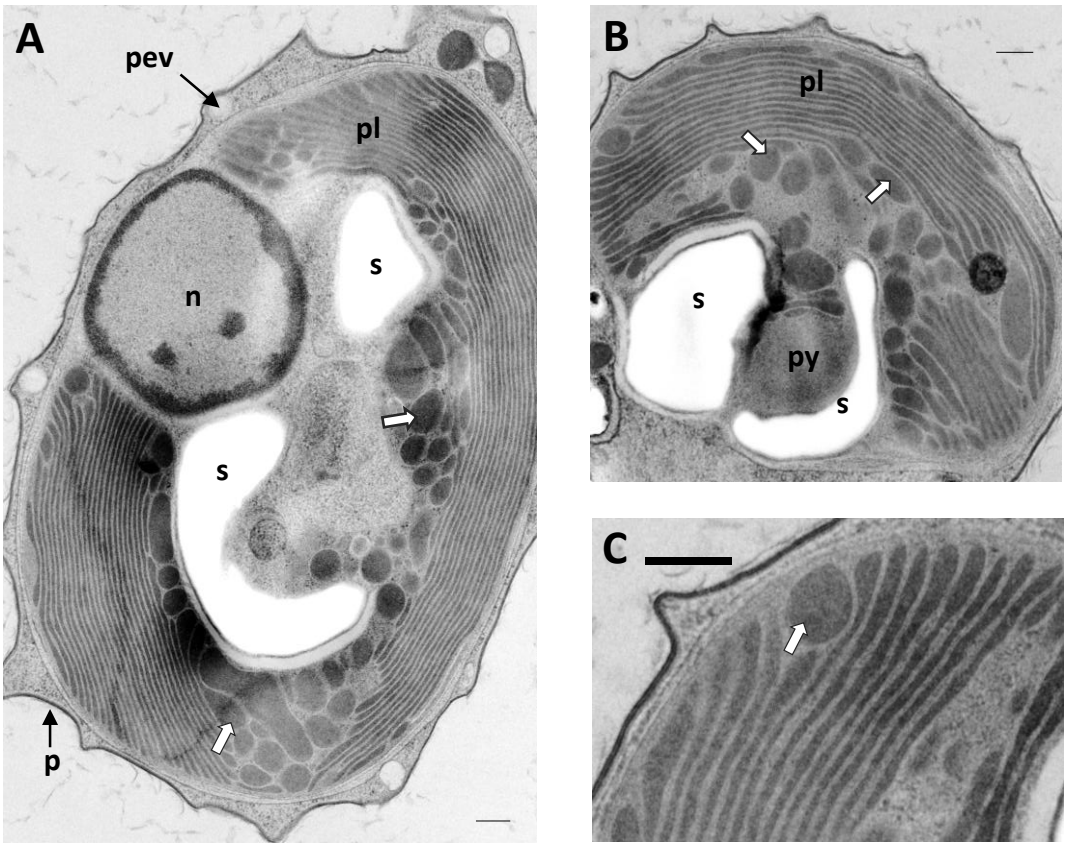

High Light

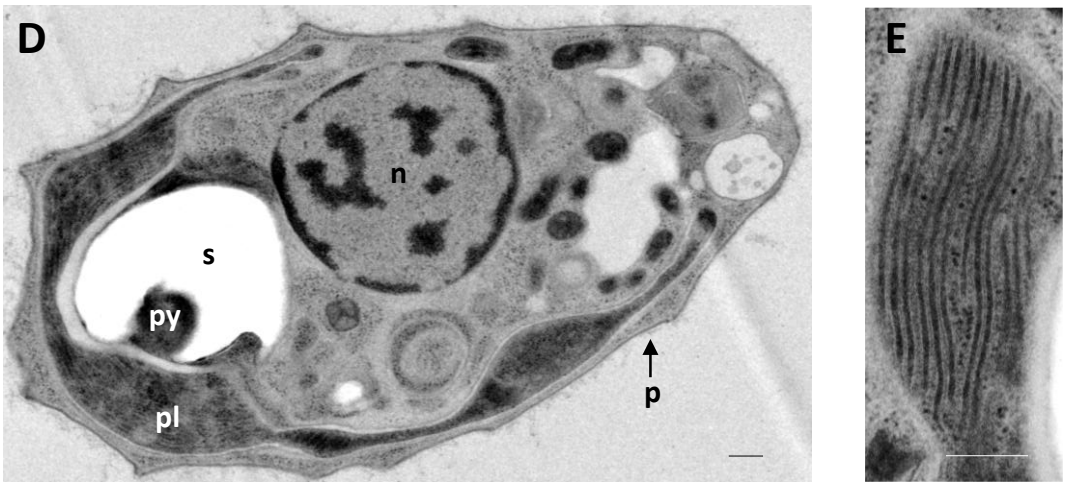

Figure 6: Transmission electron microscopy micrographs of the haploid *Teleaulax amphioxeia* Cr10EHU cells grown at 20 (**A**, **B**, **C**) and 200 (**D**, **E**) µmol photons m^{-2} s^{-1}. Cell section at the nucleus level, showing a global view of the belt-shaped low light acclimated plastid (**A**), transverse section at the pyrenoid level (**B**) and close-up on the swelling extremities of non-

clustered thylakoids forming vesicles (**C**). Section of a representative high light acclimated cell, showing the thin plastid localized against the plasma membrane (**D**) and close-up on the thinner thylakoids sometimes clustered in sets of three (**E**). **n**: nucleus; **p**: plate; **pev**: peripheral ejectosome vesicle; **pl**: plastid; **py**; pyrenoid; **s**: starch. White arrows show the thylakoidal vesicles.

Discussion

Cryptophyte microalgae are abundant and remarkably ubiquitous microalgae (see e.g. (Caracciolo et al., 2022; Pierella Karlusich et al., 2020; Xin et al., 2023). Despite their indisputable ecological significance, these organisms have been largely understudied compared to other phytoplankton groups and their light niches remain inadequately comprehended. In this study, we provide an extensive characterization of the photoacclimation mechanisms of the haploid form of the cryptophyte *Teleaulax amphioxeia*, strain Cr10EHU. This cryptophyte belongs to the so-called PTG clade (Fig. 1) that encompasses *Plagioselmis*/*Teleaulax* and *Geminigera* species. *Plagioselmis* and *Teleaulax* have been shown to be the haploid and diploid form of the same organism (Altenburger et al., 2020). While *Geminigera* appears to form a well-defined radiation (Daugbjerg et al., 2018; clades IV and VII *sensu* Hamilton et al., 2021), *Plagioselmis*/*Teleaulax* sequences are dispersed in at least 8 clades, which may correspond to different species. The haploid *Teleaulax amphioxeia* Cr10EHU falls within clade II, alongside representative sequences of the diploid form of *Teleaulax amphioxeia*, then supporting the conclusions of Altenburger et al. (2020). Another sequence of the haploid form lies at the basis of this group, hinting at a greater genetic diversity than currently represented. It is worth noting that the sequences within this clade have been sourced from organisms inhabiting the Atlantic and Pacific oceans (Table S1), underscoring the widespread prevalence of *Teleaulax amphioxeia*.

Adaptation to light niches

Cryptophytes have been often considered as adapted to low light environments due to their potential competitivity in such habitats (Bergmann, 2004; Ilmavirta, 1988) and because they use phycobiliproteins harvesting green light (for a review, see Hoef-Emden and Archibald, 2017), which is abundant in deep coastal waters. It is however widely acknowledged that seawater spectral quality varies significantly across offshore-to-coast gradients, irrespective of depth, with oceanic waters characterized by abundant blue light, whereas coastal and estuarine waters predominantly exhibit green to orange wavelengths. Marine cryptophytes are scarce in oceanic waters and primarily inhabit coastal and estuarine environments, and it is not surprising that they are optically adapted to green coastal waters. This adaptive process is well exemplified by marine *Synechococcus*, whose PE have evolved to match light spectral quality of seawater over extensive offshore to coast gradients (Grébert et al., 2018). These picocyanobacteria primarily inhabit surface waters, characterized by the

highest light levels, and exhibit optimal growth under intense light irradiance (Kana and Glibert, 1987; Moore et al., 1995; Six et al., 2004). Hence, for coastal marine *Synechococcus*, the efficient utilization of green light primarily arises from their adaptation to the offshore-coastal light quality gradient, rather than being associated to low-light niches. In addition, the presence of phycobiliproteins specialized in harvesting orange to red wavelengths in both estuarine cryptophytes and *Synechococcus* (Cunningham et al., 2019; Fuller et al., 2003; Six et al., 2007) further supports the idea that the wavelength preferences of cryptophytes may primarily be related to the light quality of coastal habitats, regardless of depth, rather than representing a specific adaptation to low-light niches.

To demonstrate evolutionary adaptation to low light niches, laboratory studies of the response to light irradiance are essential for identifying adaptive physiological traits. The present study shows that, in our culture conditions, *Teleaulax amphioxeia* Cr10EHU exhibits optimal growth at about 200 µmol photons m^{-2} s^{-1}. Comparisons with other studies shows that, in fact, various cryptophyte strains exhibit high growth rate under high light irradiance. For instance, a *Cryptomonas* strain showed a very similar growth response to *Teleaulax amphioxeia* Cr10EHU (Weng et al., 2009). The model cryptophyte *Guillardia theta* and *Rhodomonas salina* show highest growth under 150-250 µmol photons m^{-2} s^{-1} (Kieselbach et al., 2018; Wirth et al., 2019; Xie et al., 2021). The AND-A0710 strain of *Teleaulax amphioxeia* and *Geminigera cryophila* strains CCMP 2564 and GEMCRY1 showed high growth under 400-550 µmol photons m^{-2} s^{-1} (Gaillard et al., 2020; Mendes et al., 2023; Trimborn et al., 2019). This contrasts with the growth response of phytoplanktonic organisms that are evolutionary adapted to low light niches, such as the low light ecotypes of the picocyanobacterium *Prochlorococcus* and strains of the green alga *Ostreococcus*. Laboratory studies have shown that these organisms usually show optimal growth far below 100 µmol photons m^{-2} s^{-1} and experience photoinhibition beyond this irradiance (Moore et al., 1998; Moore and Chisholm, 1999; Six et al., 2007). Therefore, on the basis of its growth-irradiance response, the haploid *Teleaulax amphioxeia* Cr10EHU, along with many other cryptophyte strains, cannot be considered as a low-light adapted organism.

<u>*Regulation of the membrane pigmentation*</u>

Teleaulax amphioxeia Cr10EHU exhibits a pigmentation including chl *a*, chl c_2, the major xanthophyll alloxanthin, and the minor carotenoids crocoxanthin and α-carotene (Cunningham et al., 2019). It should be noted that *Teleaulax amphioxeia* Cr10EHU is one of the rare cryptophyte strains devoid of monadoxanthin and that our study evidenced the presence of two *cis*-xanthophylls, which appear to be common but uncharacterized in cryptophyte chromatograms (see e.g. Rial et al., 2013; Roy et al., 2011; Zapata et al., 2000). The keto-carotenoid canthaxanthin was not detected in the

haploid *Teleaulax amphioxeia* Cr10EHU, in contrast to the model cryptophyte *Guillardia theta* (Roy et al., 2011).

These pigments are bound to both PSI and PSII, encompassing their respective surrounding LHC proteins. The cryptophytes LHC bind chl *a*, chl *c* and at least three xanthophylls (Bathke et al., 1999; Kuthanová Trsková et al., 2019; Zhao et al., 2023). Chl *a* molecules are located in both the reaction centers and the LHC proteins. The observed decrease in chl *a* cell content in response to increasing growth light, thus indicates a general downregulation of the content in PS with increasing growth irradiance. This is a classical acclimation process by which photosynthetic organisms acclimate to incident light in order to optimize light utilization at low irradiance, and limit photoinhibition at high irradiance. This response can be linked to a decrease of the thylakoidal surface per plastid and/or of the concentration of PS in the thylakoids.

Carotene molecules are usually much more abundant in the reaction centers than in LHC proteins (Telfer, 2005; Zhao et al., 2023). Therefore, the 28% decrease in the α-carotene cell content in response to increasing growth irradiance indicates a specific downregulation of the content in reaction centers. Chl c_2 molecules, generally exclusively located in the LHC proteins (Zhao et al., 2023), have been shown to efficiently transfer energy to chl *a* in cryptophyte LHC complexes, confirming their light harvesting function (Šebelík et al., 2020). The large difference in chl c_2 cell content between cultures acclimated to 40 and 200 µmol photons m^{-2} s^{-1} demonstrate a dynamic regulation of the LHC proteins. Furthermore, the mass ratio chl c_2 to α-carotene, which decreased from 5 at 40 µmol photons m^{-2} s^{-1} to 3 at 200 µmol photons m^{-2} s^{-1} (Fig. S2). This suggests that the number of LHC proteins per reaction center was higher at low growth irradiance, pointing to a regulation of the size of the LHC antenna, probably involving a regulation of specific *lhc* genes. It is worth noting that the variations in crocoxanthin were almost identical to those of chl c_2. Despite there are a few crocoxanthin molecules bound to reaction center I (Zhao et al., 2023), this suggests that most of the crocoxanthins are located on the same LHC proteins with a similar chl c_2 to crocoxanthin ratio, hinting at a light harvesting function for this xanthophyll.

The study of the structure of the PSI of *Chroomonas placoidea* showed that 93% of the alloxanthin molecules are located in the LHCI proteins (Zhao et al., 2023), and a similar situation would be expected for PSII. The precise function of alloxanthin in cryptophyte LHC complexes is still poorly understood (Šebelík et al., 2020). Some works suggested a photoprotective role because the alloxanthin to chl *a* ratio was higher under high light (Funk et al., 2011; García-Portela et al., 2018; Schluter et al., 2006). However, in these studies, it was often difficult to separate the expected light-induced decrease of chl *a* from a potential increase in alloxanthin (Mendes et al., 2023). Our results show that, in the haploid *Teleaulax amphioxeia* Cr10EHU, the alloxanthin cell content clearly decreased in response to increasing growth irradiances, regardless of the chl *a* variations. This would

be compatible with a light-harvesting function for alloxanthin. On the other hand, it is worth noting that the alloxanthin to chl c_2 mass ratios increased from 1.9 at 40 µmol photons m^{-2} s^{-1} to 4 at 200 µmol photons m^{-2} s^{-1} (Fig. S2). This indicates that there are twice more alloxanthins per LHC proteins at high growth irradiance, which could be compatible with a photoprotective function. More research is necessary to ascertain the precise role of the major carotenoid of the cryptophytes.

We detected two *cis*-xanthophylls that responded differently to growth irradiance: the unk1 remained stable while unk2 exhibited an increasing trend. It should be noted that the data's variability, resulting from the relatively low quantity of the latter pigment in the cells, hinders a definitive interpretation. However, the ratio unk2 to chl c_2 shows a large increase, from 0.02 to about 0.25, with increasing growth light (Fig. S2). Unless this compound is a biosynthetic intermediate molecule, this suggests an enrichment of the LHC in unk2 in response to high growth irradiance, which might be associated to a photoprotective function.

Phycoerythrin regulation

In addition to their intrinsic LHC proteins, cryptophytes also employ luminal phycobiliproteins to capture light. The different lineages of cryptophytes have evolved various chromophorylated phycobiliproteins that absorb light in the green to orange region of the spectrum, while LHC proteins are efficient at capturing blue light. In cryptophytes from the PTG clade, including *Teleaulax amphioxeia* Cr10EHU, the specific phycobiliprotein used is PE-545 (Richardson, 2022; Fig. S3), which possesses an $\alpha\alpha'\beta_2$ closed quaternary structure and binds 2 15,16-dihydrobiliverdin and 6 phycoerythrobilin chromophores (Michie et al., 2023). Our results demonstrate that the haploid *Teleaulax amphioxeia* Cr10EHU regulates this antenna very efficiently in response to growth light irradiance, as the cell content of PE-545 varied by a factor of 4 between low and high light conditions. It is likely that this is not the maximal amplitude since the curve did not exhibit any stable region in the low and high irradiance areas, unlike the membrane pigments. These PE content changes translated in significant variations in the PSII absorption cross-section for green light, $\sigma(II)_{540nm}$, and in the slope α of the ETR/I curves, allowing the cell to efficiently tune the optimal irradiance, I_{OPT}, for the functioning of the photosynthetic machinery. Considering the high content and flexibility of PE-545, there is no doubt that this protein serves as the major antenna component of the photosynthetic antenna of the haploid *Teleaulax amphioxeia* Cr10EHU, making this cryptophyte a green light specialist. We further investigated the short-term capacity of *Teleaulax amphioxeia* Cr10EHU to regulate absorption of green light. To achieve this, we assessed photoacclimation rates by monitoring changes in $\sigma(II)_{540nm}$, during transition experiments to various lower light levels. The results showed that *Teleaulax amphioxeia* Cr10EHU could exponentially increase its antenna

photoacclimation rate in response to decreasing irradiance levels, further underscoring the remarkable adaptability of this strain to acclimate effectively to varying light intensities.

Studying the light-induced changes in plastid ultrastructure provided insights into the potential mechanisms underlying PE regulation in the haploid *Teleaulax amphioxeia* Cr10EHU. First of all, the plastid exhibited a much larger size under low light conditions than under high light ones. This allows the cell to considerably increase the number of thylakoids and support the conclusions of the membrane pigment analyses. Several studies have described the diploid forms of *Teleaulax* species, i.e. lacking hexagonal plates, as having thylakoids grouped loosely in sets of three (see e.g. Hill, 1991; Laza-Martínez et al., 2012). In the descriptive studies of the haploid '*Plagioselmis prolonga*', when it was considered a species, there is no mention of the thylakoid structure (Novarino, 2005) and the early descriptions do not offer a clear examination of this characteristic (Novarino, 2003; Novarino et al., 1994). In our study, we could observe a thylakoid clustering by sets of 3 only in cells of the haploid *Teleaulax amphioxeia* Cr10EHU. Interestingly, we observed that in cells acclimated to low growth irradiance, the thylakoid extremities tended to swell, eventually forming large independent vesicles in the inner part of the plastid. These structures appear to contain a significant amount of PE. In high light acclimated cells, the thylakoids were thinner and formed many less vesicles. Although the high volume to surface ratio of the thylakoidal vesicles might induce some packaging effect, the formation of these thylakoidal vesicles likely represent a low light acclimation trait that substantially enhances green light harvesting under low light irradiance.

Non-photochemical quenching of fluorescence in Teleaulax amphioxeia *Cr10EHU*

The study of NPQ induction upon successive steps of increasing instantaneous irradiance revealed, in the haploid *Teleaulax amphioxeia* Cr10EHU, the presence of at least two distinct NPQ components in these experiments (Fig. S4). Firstly, in dark-acclimated samples, the PSII quantum yield was not maximal and kept increasing until irradiances of 20-30 µmol photons m^{-2} s^{-1}. This process, which can be quantified as an NPQ component induced in the dark and relaxing under low incident light, resembles the so-called state transition mechanisms that occur, for instance, in the model green alga *Chlamydomonas* and in many phycobilisome-containing cyanobacteria. In green algae, the precise process has been explained by the energetic disconnection of LHC proteins from PSII, physically moving to PSI (Minagawa, 2011). In phycobilisome-containing cyanobacteria, which do not have LHC proteins, the detail of the mechanism is still subject of debate (Calzadilla and Kirilovsky, 2020). Overall, the state transition mechanism is generally interpreted as a means to regulate the delivery of light energy between both photosystems in order to optimize photosynthesis.

To study this process in the haploid *Teleaulax amphioxeia* Cr10EHU, we used the NPQ_{ST} parameter calculated between the maximal fluorescence level in the dark acclimated state and the absolute maximum fluorescence level. Our results show that the amplitude of the state transition process increases in response to higher growth light irradiance. This can be interpreted as a means of photoprotection by minimizing the PSII antenna size, in order to decrease PSII photoinactivation rate (Minagawa, 2011). The state transition mechanisms in cryptophytes has been studied in *Guillardia theta* cultures (Cheregi et al., 2015). The mechanism, which was inhibited in stationary growth phase, was activated by blue-light and much less under green light, suggesting that it was operated by the LHC proteins and not by PE-545, possibly through a phosphorylation reaction (Janssen and Rhiel, 2008). We analyzed the state transition response under blue and green light and in stationary growth phase (Fig. S5), and we found similar results with *Teleaulax amphioxeia* Cr10EHU, supporting and generalizing Cheregi et al. (2015) conclusions in *Guillardia theta*.

Several cryptophyte strains have been shown to exhibit effective and flexible non-photochemical quenching of fluorescence. For example, Kaňa et al. (2012) characterized a fast delta-pH dependent Q_E-like component of the NPQ in *Rhodomonas salina*, activated under strong high light stress inducing the saturation of the Calvin cycle, and which was proposed to occur in the LHC complexes (Giovagnetti and Ruban, 2018; Kaňa, 2018; Kaňa et al., 2012). In addition, Funk et al. (2011) and Cheregi et al., (2015) showed that a similar NPQ induction occurs in *Guillardia theta*, also in response to abrupt light stress and when reaching stationary phase. Indeed, when growth is halted and consequently the cells receive more light than they can use, aged cultures often downregulate the antenna system and induce light dissipation mechanisms. Our results show that *Teleaulax amphioxeia* Cr10EHU can also induce a Q_E-like NPQ mechanism. However, in contrast to previous works that used cultures acclimated to low light, we show here that this process can be a permanent response to growth irradiance and that its amplitude is associated to a given photoacclimation state. In vascular plants, green and brown algae, the activation of the Q_E component of NPQ requires the conversion of violaxanthin to zeaxanthin by xanthophyll de-epoxidase enzymes, a process termed xanthophyll cycle (Lacour et al., 2020). In many chl *c*-containing microalgae, this mechanism often involves the conversion of diadinoxanthin to diatoxanthin, but none of these pigments are present in cryptophytes. The molecular mechanisms underlying NPQ in cryptophytes still remain elusive. Our study however shows that the LHC in high light acclimated cells is enriched in alloxanthin (see above) and maybe in the unk2 xanthophyll, a process that might be linked to the NPQ mechanism.

Conclusion

Cryptophytes of the species *Teleaulax amphioxeia* are abundant and widely distributed microalgae in coastal oceans. Our study reveals that, similar to many other cryptophyte strains, the haploid form *Teleaulax amphioxeia* Cr10EHU can thrive under a broad range of light irradiances. To achieve this, this organism adjusts finely the cell pigment composition to regulate light utilization. Particularly noteworthy is the substantial variability in the cell content of the major green light antenna, PE-545, which relies on the formation of thylakoidal vesicles, a process previously unreported. Additionally, we demonstrate that the rate at which the size of the PE antenna acclimates is dependent on the amplitude of the variations in irradiance, rendering this organism highly flexible from a photophysiological perspective. Furthermore, *Teleaulax amphioxeia* Cr10CHU employs different NPQ processes that, although their functioning remains unknown, are likely key to regulate light utilization under different light conditions.

Teleaulax amphioxeia serves as an efficient plastid donor to the red-tide forming ciliate *Mesodinium rubrum* and toxic dinoflagellates belonging to the *Dinophysis* genus. Understanding the physiological capabilities of the plastid within its native host is essential for gaining insights into the light utilization processes of *Mesodinium* and *Dinophysis* species. Specifically, *Mesodinium rubrum* is known for its extensive vertical migrations, exposing the plastids to significant fluctuations in irradiance. The photophysiological adaptability of the plastid in *Teleaulax amphioxeia*, as highlighted in this study, aligns with the lifestyle of *Mesodinium rubrum* and is likely a prerequisite for sustaining the kleptoplastidy process. Our study constitutes a comprehensive photophysiological characterization of the haploid form of *Teleaulax amphioxeia*, strain Cr10EHU, which will be useful in future laboratory studies of the kleptoplastidy process.

Acknowlegdments

We warmly thank Aitor Laza-Martinez, the isolator of this strain, for giving access to the culture and the isolation information. We are grateful to José Garrido for his expertise in interpreting HPLC chromatograms. This study was funded by the CRYPTONIT Emergence program of Sorbonne University (Paris) and the association of European marine biological laboratories expanded (ASSEMBLE+). Sarah Garric's work is supported by the Institut de l'Océan of Sorbonne University.

→ Projets de Fran, Ian & Johan à remercier

References

Altenburger, A., Blossom, H.E., Garcia-Cuetos, L., Jakobsen, H.H., Carstensen, J., Lundholm, N., Hansen, P.J., Moestrup, Ø., Haraguchi, L., 2020. Dimorphism in cryptophytes—The case of *Teleaulax amphioxeia* / *Plagioselmis prolonga* and its ecological implications. Sci. Adv. 6, eabb1611. https://doi.org/10.1126/sciadv.abb1611

609 Archibald, J.M., 2015. Genomic perspectives on the birth and spread of plastids. Proc. Natl. Acad. Sci. 112,
610 10147–10153. https://doi.org/10.1073/pnas.1421374112

611 Bathke, L., Rhiel, E., Krumbein, W.E., Marquardt, J., 1999. Biochemical and Immunochemical Investigations on
612 the Light-Harvesting System of the Cryptophyte *Rhodomonas* sp.: Evidence for a Photosystem I
613 Specific Antenna. Plant Biol. 1, 516–523. https://doi.org/10.1111/j.1438-8677.1999.tb00777.x

614 Baurain, D., Brinkmann, H., Petersen, J., Rodriguez-Ezpeleta, N., Stechmann, A., Demoulin, V., Roger, A.J.,
615 Burger, G., Lang, B.F., Philippe, H., 2010. Phylogenomic Evidence for Separate Acquisition of Plastids in
616 Cryptophytes, Haptophytes, and Stramenopiles. Mol. Biol. Evol. 27, 1698–1709.
617 https://doi.org/10.1093/molbev/msq059

618 Bergmann, T., 2004. Impacts of a recurrent resuspension event and variable phytoplankton community
619 composition on remote sensing reflectance. J. Geophys. Res. 109, C10S15.
620 https://doi.org/10.1029/2002JC001575

621 Büchel, C., 2020. Light harvesting complexes in chlorophyll c-containing algae. Biochim. Biophys. Acta BBA -
622 Bioenerg. 1861, 148027. https://doi.org/10.1016/j.bbabio.2019.05.003

623 Calzadilla, P.I., Kirilovsky, D., 2020. Revisiting cyanobacterial state transitions. Photochem. Photobiol. Sci. 19,
624 585–603. https://doi.org/10.1039/c9pp00451c

625 Caracciolo, M., Rigaut-Jalabert, F., Romac, S., Mahé, F., Forsans, S., Gac, J., Arsenieff, L., Manno, M., Chaffron,
626 S., Cariou, T., Hoebeke, M., Bozec, Y., Goberville, E., Le Gall, F., Guilloux, L., Baudoux, A., De Vargas, C.,
627 Not, F., Thiébaut, E., Henry, N., Simon, N., 2022. Seasonal dynamics of marine protist communities in
628 tidally mixed coastal waters. Mol. Ecol. 31, 3761–3783. https://doi.org/10.1111/mec.16539

629 Cerino, F., Zingone, A., 2007. Decrypting cryptomonads: a challenge for molecular taxonomy, in: Unravelling
630 the Algae: The Past, Present, and Future of Algal Systematics, The Systematics Association Special
631 Volume Series. pp. 197–214.

632 Cheregi, O., Kotabová, E., Prášil, O., Schröder, W.P., Kaňa, R., Funk, C., 2015. Presence of state transitions in the
633 cryptophyte alga *Guillardia theta*. J. Exp. Bot. 66, 6461–6470. https://doi.org/10.1093/jxb/erv362

634 Clay, B.L., Kugrens, P., Lee, R.E., 1999. A revised classification of Cryptophyta. Bot. J. Linn. Soc. 131, 131–151.
635 https://doi.org/10.1111/j.1095-8339.1999.tb01845.x

636 Cunningham, B.R., Greenwold, M.J., Lachenmyer, E.M., Heidenreich, K.M., Davis, A.C., Dudycha, J.L.,
637 Richardson, T.L., 2019. Light capture and pigment diversity in marine and freshwater cryptophytes. J.
638 Phycol. 55, 552–564. https://doi.org/10.1111/jpy.12816

639 Daugbjerg, N., Norlin, A., Lovejoy, C., 2018. *Baffinella frigidus* gen. et sp. nov. (Baffinellaceae fam. nov.,
640 Cryptophyceae) from Baffin Bay: Morphology, pigment profile, phylogeny, and growth rate response
641 to three abiotic factors. J. Phycol. 54, 665–680. https://doi.org/10.1111/jpy.12766

642 de Vargas, C., Audic, S., Henry, N., Decelle, J., Mahe, F., Logares, R., Lara, E., Berney, C., Le Bescot, N., Probert,
643 I., Carmichael, M., Poulain, J., Romac, S., Colin, S., Aury, J.-M., Bittner, L., Chaffron, S., Dunthorn, M.,
644 Engelen, S., Flegontova, O., Guidi, L., Horak, A., Jaillon, O., Lima-Mendez, G., Luke, J., Malviya, S.,
645 Morard, R., Mulot, M., Scalco, E., Siano, R., Vincent, F., Zingone, A., Dimier, C., Picheral, M., Searson,
646 S., Kandels-Lewis, S., Tara Oceans Coordinators, Acinas, S.G., Bork, P., Bowler, C., Gorsky, G., Grimsley,
647 N., Hingamp, P., Iudicone, D., Not, F., Ogata, H., Pesant, S., Raes, J., Sieracki, M.E., Speich, S.,
648 Stemmann, L., Sunagawa, S., Weissenbach, J., Wincker, P., Karsenti, E., Boss, E., Follows, M., Karp-
649 Boss, L., Krzic, U., Reynaud, E.G., Sardet, C., Sullivan, M.B., Velayoudon, D., 2015. Eukaryotic plankton
650 diversity in the sunlit ocean. Science 348, 1261605–1261605.
651 https://doi.org/10.1126/science.1261605

652 Deane, J.A., Strachan, I.M., Saunders, G.W., Hill, D.R.A., McFadden, G.I., 2002. Cryptomonad evolution: nucelar
653 18S rDNA phylogeny versus cell morphology and pigmentation. J. Phycol. 38, 1236–1244.
654 https://doi.org/10.1046/j.1529-8817.2002.01250.x

655 Eilers, P.H.C., Peeters, J.C.H., 1988. A model for the relationship between light intensity and the rate of
656 photosynthesis in phytoplankton. Ecol. Model. 42, 199–215. https://doi.org/10.1016/0304-
657 3800(88)90057-9

Fuller, N.J., Marie, D., Partensky, F., Vaulot, D., Post, A.F., Scanlan, D.J., 2003. Clade-Specific 16S Ribosomal DNA Oligonucleotides Reveal the Predominance of a Single Marine *Synechococcus* Clade throughout a Stratified Water Column in the Red Sea. Appl. Environ. Microbiol. 69, 2430–2443. https://doi.org/10.1128/AEM.69.5.2430-2443.2003

Funk, C., Alami, M., Tibiletti, T., Green, B.R., 2011. High light stress and the one-helix LHC-like proteins of the cryptophyte *Guillardia theta*. Biochim. Biophys. Acta BBA - Bioenerg. 1807, 841–846. https://doi.org/10.1016/j.bbabio.2011.03.011

Gaillard, S., Charrier, A., Malo, F., Carpentier, L., Bougaran, G., Hégaret, H., Réveillon, D., Hess, P., Séchet, V., 2020. Combined Effects of Temperature, Irradiance, and pH on *Teleaulax amphioxeia* (Cryptophyceae) Physiology and Feeding Ratio For Its Predator *Mesodinium rubrum* (Ciliophora). J. Phycol. 56, 775–783. https://doi.org/10.1111/jpy.12977

García-Portela, M., Riobó, P., Reguera, B., Garrido, J.L., Blanco, J., Rodríguez, F., 2018. Comparative ecophysiology of *Dinophysis acuminata* and *D. acuta* (DINOPHYCEAE, DINOPHYSIALES): effect of light intensity and quality on growth, cellular toxin content, and photosynthesis. J. Phycol. 54, 899–917. https://doi.org/10.1111/jpy.12794

Giovagnetti, V., Ruban, A.V., 2018. The evolution of the photoprotective antenna proteins in oxygenic photosynthetic eukaryotes. Biochem. Soc. Trans. 46, 1263–1277. https://doi.org/10.1042/BST20170304

Grébert, T., Doré, H., Partensky, F., Farrant, G.K., Boss, E.S., Picheral, M., Guidi, L., Pesant, S., Scanlan, D.J., Wincker, P., Acinas, S.G., Kehoe, D.M., Garczarek, L., 2018. Light color acclimation is a key process in the global ocean distribution of *Synechococcus* cyanobacteria. Proc. Natl. Acad. Sci. 115, E2010–E2019. https://doi.org/10.1073/pnas.1717069115

Greenwold, M.J., Cunningham, B.R., Lachenmyer, E.M., Pullman, J.M., Richardson, T.L., Dudycha, J.L., 2019. Diversification of light capture ability was accompanied by the evolution of phycobiliproteins in cryptophyte algae. Proc. R. Soc. B Biol. Sci. 286, 20190655. https://doi.org/10.1098/rspb.2019.0655

Guillard, R.R.L., Hargraves, P.E., 1993. *Stichochrysis immobilis* is a diatom, not a chrysophyte. Phycologia 32, 234–236.

Hall, T.A., 2007. BioEdit: a user-friendly biological sequence alignment editor and analysis program for Windows 95/98/NT. Nucleic Acids Symp. Ser. 41, 95–98.

Hamilton, M., Mascioni, M., Hehenberger, E., Bachy, C., Yung, C., Vernet, M., Worden, A.Z., 2021. Spatiotemporal Variations in Antarctic Protistan Communities Highlight Phytoplankton Diversity and Seasonal Dominance by a Novel Cryptophyte Lineage. mBio 12, e02973-21. https://doi.org/10.1128/mBio.02973-21

Hansen, P., Moldrup, M., Tarangkoon, W., Garcia-Cuetos, L., Moestrup, Ø., 2012. Direct evidence for symbiont sequestration in the marine red tide ciliate *Mesodinium rubrum*. Aquat. Microb. Ecol. 66, 63–75. https://doi.org/10.3354/ame01559

Hansen, P.J., Nielsen, L.T., Johnson, M., Berge, T., Flynn, K.J., 2013. Acquired phototrophy in *Mesodinium* and *Dinophysis* – A review of cellular organization, prey selectivity, nutrient uptake and bioenergetics. Harmful Algae 28, 126–139. https://doi.org/10.1016/j.hal.2013.06.004

Hill, D.R.A., 1991. A revised circumscription of Cryptomonas (Cryptopbyceae) based on examination of Australian strains. Phycologia 30, 170–188.

Hoef-Emden, K., Archibald, J.M., 2017. Cryptophyta (Cryptomonads), in: Archibald, J.M., Simpson, A.G.B., Slamovits, C.H. (Eds.), Handbook of the Protists. Springer International Publishing, Cham, pp. 851–891. https://doi.org/10.1007/978-3-319-28149-0_35

Ilmavirta, V., 1988. Phytoflagellates and their ecology in Finnish brown-water lakes. Hydrobiologia 161, 255–270.

Janssen, J., Rhiel, E., 2008. Evidence of monomeric photosystem I complexes and phosphorylation of chlorophyll a/c-binding polypeptides in *Chroomonas* sp. strain LT (Cryptophyceae). Int. Microbiol. 11, 171–178.

Kaňa, R., 2018. Application of spectrally resolved fluorescence induction to study light-induced nonphotochemical quenching in algae. Photosynthetica 56, 132–138. https://doi.org/10.1007/s11099-018-0780-1

Kaňa, R., Kotabová, E., Sobotka, R., Prášil, O., 2012. Non-Photochemical Quenching in Cryptophyte Alga *Rhodomonas salina* Is Located in Chlorophyll a/c Antennae. PLoS ONE 7, e29700. https://doi.org/10.1371/journal.pone.0029700

Kana, T.M., Glibert, P.M., 1987. Effect of irradiances up to 2000 µE m-2 s-1 on marine *Synechococcus* WH7803 - I. Growth, pigmentation and cell composition. Deep-Sea Res. 34, 479–495.

Keeling, P.J., 2013. The Number, Speed, and Impact of Plastid Endosymbioses in Eukaryotic Evolution. Annu. Rev. Plant Biol. 64, 583–607. https://doi.org/10.1146/annurev-arplant-050312-120144

Kereïche, S., Kouřil, R., Oostergetel, G.T., Fusetti, F., Boekema, E.J., Doust, A.B., Van Der Weij-de Wit, C.D., Dekker, J.P., 2008. Association of chlorophyll a/c2 complexes to photosystem I and photosystem II in the cryptophyte *Rhodomonas* CS24. Biochim. Biophys. Acta BBA - Bioenerg. 1777, 1122–1128. https://doi.org/10.1016/j.bbabio.2008.04.045

Kieselbach, T., Cheregi, O., Green, B.R., Funk, C., 2018. Proteomic analysis of the phycobiliprotein antenna of the cryptophyte alga *Guillardia theta* cultured under different light intensities. Photosynth. Res. 135, 149–163. https://doi.org/10.1007/s11120-017-0400-0

Koike, K., Takishita, K., 2008. Anucleated cryptophyte vestiges in the gonyaulacalean dinoflagellates *Amylax buxus* and *Amylax triacantha* (Dinophyceae). Phycol. Res. 56, 301–311. https://doi.org/10.1111/j.1440-1835.2008.00512.x

Kumar, S., Stecher, G., Li, M., Knyaz, C., Tamura, K., 2018. MEGA X: Molecular Evolutionary Genetics Analysis across Computing Platforms. Mol Biol Evol. Mol. Biol. Evol. 35, 1547–1549.

Kuthanová Trsková, E., Bína, D., Santabarbara, S., Sobotka, R., Kaňa, R., Belgio, E., 2019. Isolation and characterization of CAC antenna proteins and photosystem I supercomplex from the cryptophytic alga *Rhodomonas salina*. Physiol. Plant. 166, 309–319. https://doi.org/10.1111/ppl.12928

Lacour, T., Babin, M., Lavaud, J., 2020. Diversity in Xanthophyll Cycle Pigments Content and Related Nonphotochemical Quenching (NPQ) Among Microalgae: Implications for Growth Strategy and Ecology. J. Phycol. 56, 245–263. https://doi.org/10.1111/jpy.12944

Laza-Martínez, A., Arluzea, J., Miguel, I., Orive, E., 2012. Morphological and molecular characterization of *Teleaulax gracilis* sp. nov. and *T. minuta* sp. nov. (Cryptophyceae). Phycologia 51, 649–661. https://doi.org/10.2216/11-044.1

Ludwig, M., Gibbs, S.P., 1989. Localization of phycoerythrin at the lumenal surface of the thylakoid membrane in *Rhodomonas lens*. J. Cell Biol. 108, 875–884. https://doi.org/10.1083/jcb.108.3.875

Marie, D., Simon, N., Vaulot, D., 2005. Phytoplankton Cell Counting by Flow Cytometry, in: Algal Culturing Techniques. Elsevier, pp. 253–267. https://doi.org/10.1016/B978-012088426-1/50018-4

Medlin, L., Elwood, H.J., Stickel, S., Sogin, M.L., 1988. The characterization of enzymatically amplified eukaryotic 16S-like rRNA-coding regions. Gene 71, 491–499. https://doi.org/10.1016/0378-1119(88)90066-2

Mendes, C.R.B., Costa, R.R., Ferreira, A., Jesus, B., Tavano, V.M., Dotto, T.S., Leal, M.C., Kerr, R., Islabão, C.A., Franco, A.D.O.D.R., Mata, M.M., Garcia, C.A.E., Secchi, E.R., 2023. Cryptophytes: An emerging algal group in the rapidly changing Antarctic Peninsula marine environments. Glob. Change Biol. 29, 1791–1808. https://doi.org/10.1111/gcb.16602

Michie, K.A., Harrop, S.J., Rathbone, H.W., Wilk, K.E., Teng, C.Y., Hoef-Emden, K., Hiller, R.G., Green, B.R., Curmi, P.M.G., 2023. Molecular structures reveal the origin of spectral variation in cryptophyte light harvesting antenna proteins. Protein Sci. 32, e4586. https://doi.org/10.1002/pro.4586

Minagawa, J., 2011. State transitions—The molecular remodeling of photosynthetic supercomplexes that controls energy flow in the chloroplast. Biochim. Biophys. Acta BBA - Bioenerg. 1807, 897–905. https://doi.org/10.1016/j.bbabio.2010.11.005

Moeller, H.V., Johnson, M.D., 2023. *Mesodinium*. Curr. Biol. 33, R249–R250. https://doi.org/10.1016/j.cub.2023.02.015

Moore, L.R., Chisholm, S.W., 1999. Photophysiology of the marine cyanobacterium *Prochlorococcus*: Ecotypic differences among cultured isolates. Limnol. Oceanogr. 44, 628–638. https://doi.org/10.4319/lo.1999.44.3.0628

Moore, L.R., Goericke, R., Chisholm, S.W., 1995. Comparative physiology of *Synechococcus* and *Prochlorococcus*: influence of light and temperature on growth, pigments, fluorescence and absorptive properties. Mar. Ecol. Prog. Ser. 116, 259–275.

Moore, L.R., Rocap, G., Chisholm, S.W., 1998. Physiology and molecular phylogeny of coexisting *Prochlorococcus* ecotypes. Nature 393, 464–467. https://doi.org/10.1038/30965

Novarino, G., 2005. Nanoplankton protists from the western Mediterranean Sea. II. Cryptomonads (Cryptophyceae = Crptomonadea). Sci. Mar. 69, 47–74. https://doi.org/10.3989/scimar.2005.69n147

Novarino, G., 2003. A companion to the identification of cryptomonad flagellates (Cryptophyceae = Cryptomonadea). Hydrobiologia 502, 225–270. https://doi.org/10.1023/B:HYDR.0000004284.12535.25

Novarino, G., Lucas, I.A.N., Morall, S., 1994. Observations on the genus *Plagioselmis* (Cryptophyceae). Cryptogam. Algol. 15, 87–107.

Park, M.G., Kim, M., Kang, M., 2013. A Dinoflagellate *Amylax triacantha* with Plastids of the Cryptophyte Origin: Phylogeny, Feeding Mechanism, and Growth and Grazing Responses. J. Eukaryot. Microbiol. 60, 363–376. https://doi.org/10.1111/jeu.12041

Peltomaa, E., Johnson, M., 2017. *Mesodinium rubrum* exhibits genus-level but not species-level cryptophyte prey selection. Aquat. Microb. Ecol. 78, 147–159. https://doi.org/10.3354/ame01809

Pennington, F.C., Haxo, F.T., Borch, G., Liaaen-Jensen, S., 1985. Carotenoids of cryptophyceae. Biochem. Syst. Ecol. 13, 215–219. https://doi.org/10.1016/0305-1978(85)90029-8

Pierella Karlusich, J.J., Ibarbalz, F.M., Bowler, C., 2020. Phytoplankton in the *Tara* Ocean. Annu. Rev. Mar. Sci. 12, 233–265. https://doi.org/10.1146/annurev-marine-010419-010706

Rathbone, H.W., Michie, K.A., Landsberg, M.J., Green, B.R., Curmi, P.M.G., 2021. Scaffolding proteins guide the evolution of algal light harvesting antennas. Nat. Commun. 12, 1890. https://doi.org/10.1038/s41467-021-22128-w

Rial, P., Garrido, J.L., Jaén, D., Rodríguez, F., 2013. Pigment composition in three *Dinophysis* species (Dinophyceae) and the associated cultures of *Mesodinium* rubrum and *Teleaulax amphioxeia*. J. Plankton Res. 35, 433–437. https://doi.org/10.1093/plankt/fbs099

Rial, P., Laza-Martínez, A., Reguera, B., Raho, N., Rodríguez, F., 2015. Origin of cryptophyte plastids in *Dinophysis* from Galician waters: results from field and culture experiments. Aquat. Microb. Ecol. 76, 163–174. https://doi.org/10.3354/ame01774

Richardson, T.L., 2022. The colorful world of cryptophyte phycobiliproteins. J. Plankton Res. 44, 806–818. https://doi.org/10.1093/plankt/fbac048

Ronquist, F., Huelsenbeck, J.P., 2003. MrBayes 3: Bayesian phylogenetic inference under mixed models. Bioinformatics 19, 1572–1574. https://doi.org/10.1093/bioinformatics/btg180

Roy, S., Llewellyn, C.A., Egeland, E.S., Johnsen, G., 2011. Phytoplankton Pigments. Characterization, Chemotaxonomy and Applications in Oceanography, Cambridge Environmental Chemistry Series. Cambridge University Press.

Schluter, L., Lauridsen, T.L., Krogh, G., Jorgensen, T., 2006. Identification and quantification of phytoplankton groups in lakes using new pigment ratios – a comparison between pigment analysis by HPLC and microscopy. Freshw. Biol. 51, 1474–1485. https://doi.org/10.1111/j.1365-2427.2006.01582.x

Schreiber, U., Klughammer, C., Kolbowski, J., 2012. Assessment of wavelength-dependent parameters of photosynthetic electron transport with a new type of multi-color PAM chlorophyll fluorometer. Photosynth. Res. 113, 127–144. https://doi.org/10.1007/s11120-012-9758-1

Šebelík, V., West, R., Trsková, E.K., Kaňa, R., Polívka, T., 2020. Energy transfer pathways in the CAC light-harvesting complex of *Rhodomonas salina*. Biochim. Biophys. Acta BBA - Bioenerg. 1861, 148280. https://doi.org/10.1016/j.bbabio.2020.148280

Six, C., Ratin, M., Marie, D., Corre, E., 2021. Marine *Synechococcus* picocyanobacteria: Light utilization across latitudes. Proc. Natl. Acad. Sci. 118, e2111300118. https://doi.org/10.1073/pnas.2111300118

Six, C., Thomas, J., Brahamsha, B., Lemoine, Y., Partensky, F., 2004. Photophysiology of the marine cyanobacterium *Synechococcus* sp. WH8102, a new model organism. Aquat. Microb. Ecol. 35, 17–29. https://doi.org/10.3354/ame035017

Six, C., Thomas, J.-C., Garczarek, L., Ostrowski, M., Dufresne, A., Blot, N., Scanlan, D.J., Partensky, F., 2007. Diversity and evolution of phycobilisomes in marine *Synechococcus* spp.: a comparative genomics study. Genome Biol. 8, R259. https://doi.org/10.1186/gb-2007-8-12-r259

Sunesen, I., Rodríguez, F., Tardivo Kubis, J.A., Aguiar Juárez, D., Risso, A., Lavigne, A.S., Wietkamp, S., Tillmann, U., Sar, E.A., 2020. Morphological and molecular characterization of *Heterocapsa claromecoensis* sp. nov. (Peridiniales, Dinophyceae) from Buenos Aires coastal waters (Argentina). Eur. J. Phycol. 55, 490–506. https://doi.org/10.1080/09670262.2020.1750059

Telfer, A., 2005. Too much light? How β-carotene protects the photosystem II reaction centre. Photochem. Photobiol. Sci. 4, 950. https://doi.org/10.1039/b507888c

Trimborn, S., Thoms, S., Karitter, P., Bischof, K., 2019. Ocean acidification and high irradiance stimulate the photo-physiological fitness, growth and carbon production of the Antarctic cryptophyte *Geminigera cryophila*. Biogeosciences 16, 2997–3008. https://doi.org/10.5194/bg-16-2997-2019

Weng, H.-X., Qin, Y.-C., Sun, X.-W., Chen, X.-H., Chen, J.-F., 2009. Effects of light intensity on the growth of *Cryptomonas* sp. (Cryptophyceae). Environ. Geol. 57, 9–15. https://doi.org/10.1007/s00254-008-1277-1

Wirth, C., Limberger, R., Weisse, T., 2019. Temperature × light interaction and tolerance of high water temperature in the planktonic freshwater flagellates *Cryptomonas* (Cryptophyceae) and *Dinobryon* (Chrysophyceae). J. Phycol. 55, 404–414. https://doi.org/10.1111/jpy.12826

Xie, J., Chen, S., Wen, Z., 2021. Effects of light intensity on the production of phycoerythrin and polyunsaturated fatty acid by microalga *Rhodomonas salina*. Algal Res. 58, 102397. https://doi.org/10.1016/j.algal.2021.102397

Xin, Q., Qin, X., Wu, G., Ding, X., Wang, X., Hu, Q., Mu, C., Wei, Y., Chen, J., Jiang, T., 2023. Phytoplankton community structure in the Western Subarctic Gyre of the Pacific Ocean during summer determined by a combined approach of HPLC-pigment CHEMTAX and metabarcoding sequencing. Front. Mar. Sci. 10, 1116050. https://doi.org/10.3389/fmars.2023.1116050

Zapata, M., Rodríguez, F., Garrido, J., 2000. Separation of chlorophylls and carotenoids from marine phytoplankton:a new HPLC method using a reversed phase C8 column and pyridine-containing mobile phases. Mar. Ecol. Prog. Ser. 195, 29–45. https://doi.org/10.3354/meps195029

Zhao, L.-S., Wang, P., Li, K., Zhang, Q.-B., He, F.-Y., Li, C.-Y., Su, H.-N., Chen, X.-L., Liu, L.-N., Zhang, Y.-Z., 2023. Structural basis and evolution of the photosystem I–light-harvesting supercomplex of cryptophyte algae. Plant Cell 35, 2449–2463. https://doi.org/10.1093/plcell/koad087